Supplementary Information to “An improved approach to estimate the natural land carbon sink”

Mike O’Sullivan et al.

Supplementary text

Variation in modelled RSS

The magnitude of RSS differs across models, not only in its global mean but also in its regional pattern. This variation reflects differences in how each of the seven DGVMs represents initial vegetation distribution, historical land cover change and its consequences for carbon fluxes, and how NBP rates of forest and non-forest plants are modelled. All models are constrained by cropland and pasture area from LUH2/HYDE, but forest areas are less tightly constrained: land cover transitions - i.e. whether agriculture expands into forests or grasslands - are handled differently by each modelling team, as is the potential vegetation map used by the DGVMs (Supplementary Table 1); both greatly influence forest cover and its changes[1–3].

Some models appear to underrepresent historical deforestation. For example, CLASSIC and VISIT simulate limited forest loss in South America (Supplementary Figure 4), which explains their minimal estimated bias (i.e. RSS) there (Supplementary Figure 3). However, multiple forest cover reconstructions (e.g. LUH2[4,5], Houghton & Castanho [6]) suggest substantial historical forest loss in this region, implying that these models likely underestimate deforestation and, thus, the bias in SLAND due to RSS.

Conversely, IBIS reproduces a strong deforestation signal in South America but shows a negative RSS bias in this region (Supplementary Figure 3). This implies that the replacement vegetation (agricultural PFTs) has a higher simulated carbon uptake than the natural forest and savannas it replaces. The IBIS result appears to be driven by climate responses: warming and drying over recent decades have led to forest dieback and declining productivity (reducing SLAND in the S2 simulation with fixed pre-industrial land cover), offsetting the expected increase in sink capacity from CO2 fertilisation. In other words, the NBP per unit forest area is lower than the NBP of the grasslands and croplands that replaced the forest (Supplementary Figure 5). Notably, IBIS stands out compared to other models in that its RSS bias does not appear to correlate with forest loss. For example, in India, a region where all other models show a clear positive RSS bias consistent with extensive agricultural expansion, IBIS simulates almost no RSS bias. This is because IBIS assumes that cropland replaces shrubs (and not forest) in that region.

In regions such as the eastern United States and parts of Southeast Asia, nearly all models show strong positive RSS biases (Figure 2 of main manuscript and Supplementary Figure 3), consistent with historical forest loss that is not accounted for in the fixed pre-industrial

land cover used in GCB simulations. Yet, even among these regions, the strength of the RSS bias differs by model, depending on how forest loss is implemented and how PFT-level productivity is scaled. For example, JSBACH simulates a large positive RSS bias in the USA due to extensive historical forest loss not counterbalanced by regrowth. The contrast between JSBACH and IBIS in forested regions illustrates that the carbon sink capacity attributed to forest vs non-forest vegetation - and the assumptions about recovery or transitions - can strongly shape modelled RSS.

Overall, forest area change is a major determinant of RSS but not the sole driver. The combination of land cover dynamics and biophysical response to climate collectively explain the variation. This complexity underlines the need for improved benchmarks of land-use maps and a better understanding of how different vegetation types respond to both historical and future environmental conditions.

Further, models use the LUH2 information differently. For instance, some treat pasture as natural grassland while others implement active grazing or crop management; some models implement wood harvest with varying decay rates; some use full land-use transition information whereas others just implement net transitions; some prescribe crops and pastures and let natural vegetation evolve freely, whereas others prescribe all PFT covers[7–9]. These implementation choices contribute to the model spread in RSS.

It is key for DGVMs to accurately represent land cover and land use changes in order to correctly simulate both SLAND and ELUC. Accurate representation of all forest types, including plantations, is increasingly important, especially as afforestation and reforestation are central to climate mitigation strategies[10]. With growing emphasis on regional and country-level carbon budgets[11], it becomes essential to align modelled land cover change with national inventory definitions[12]. Failure to include managed forests and plantations in driving datasets and models may systematically underestimate the natural land sink in regions pursuing aggressive forest restoration policies[13]. This underscores the need to expand and refine land-use datasets and to ensure that key land cover transitions, including plantation dynamics, are appropriately represented in both models and the datasets that drive them.

Supplementary tables

Table S1 - Initial tree cover (Million km2) for large countries. Data is taken from the first year of the S2 simulation used to estimate SLAND.

	CABLE-POP	CLASSIC	IBIS	JSBACH	LPX	OCN	VISIT
Brazil	6.84	5.5	6.42	5.47	7.39	6	5.7
Indonesia	1.6	1.01	1.63	1.31	1.75	1.34	1.68
India	1.64	0.96	0.5	1.66	0.91	1.9	1.37
China	3.46	2.4	3.59	2.95	4.15	3.01	2.98
United States of America	5.19	3.31	4.25	3.91	4.88	5.03	4.18
Russia	9.98	9.08	9.34	8.31	11.16	9.83	11.91

Supplementary figures

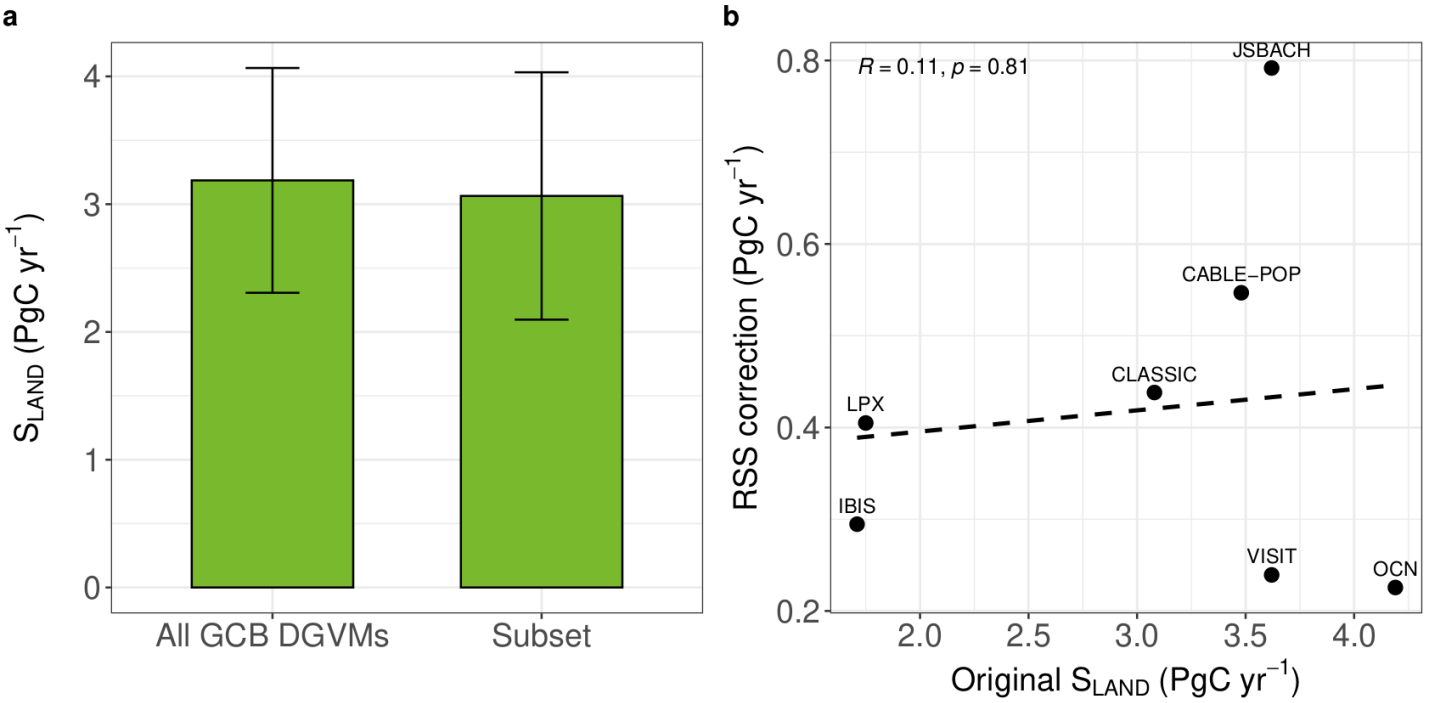

Supplementary Figure 1 - (a) Comparison of SLAND from the full GCB2024 DGVM ensemble (n=20) and the subset used in our correction (n=7), averaged over 2014-2023. The similarity in ensemble means and standard deviations supports the validity of applying the RSS correction directly to the GCB SLAND estimate. (b) Relationship between the original SLAND values and the RSS correction across the subset of seven models.

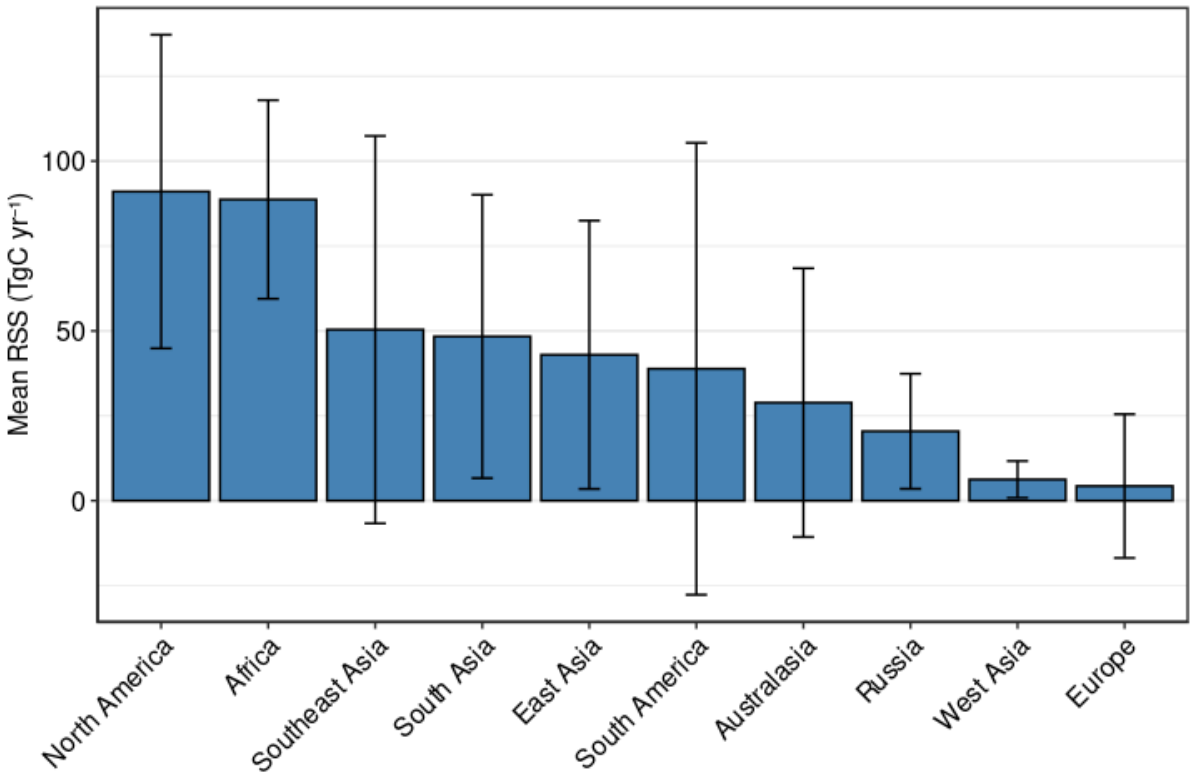

Supplementary Figure 2 - Mean regional RSS averaged over 2014-2023 for RECCAP2 regions. The regions are shown in Figure 2 in the main manuscript. Bars show the mean across the seven DGVMs used and the model spread (1σ) is shown with error bars.

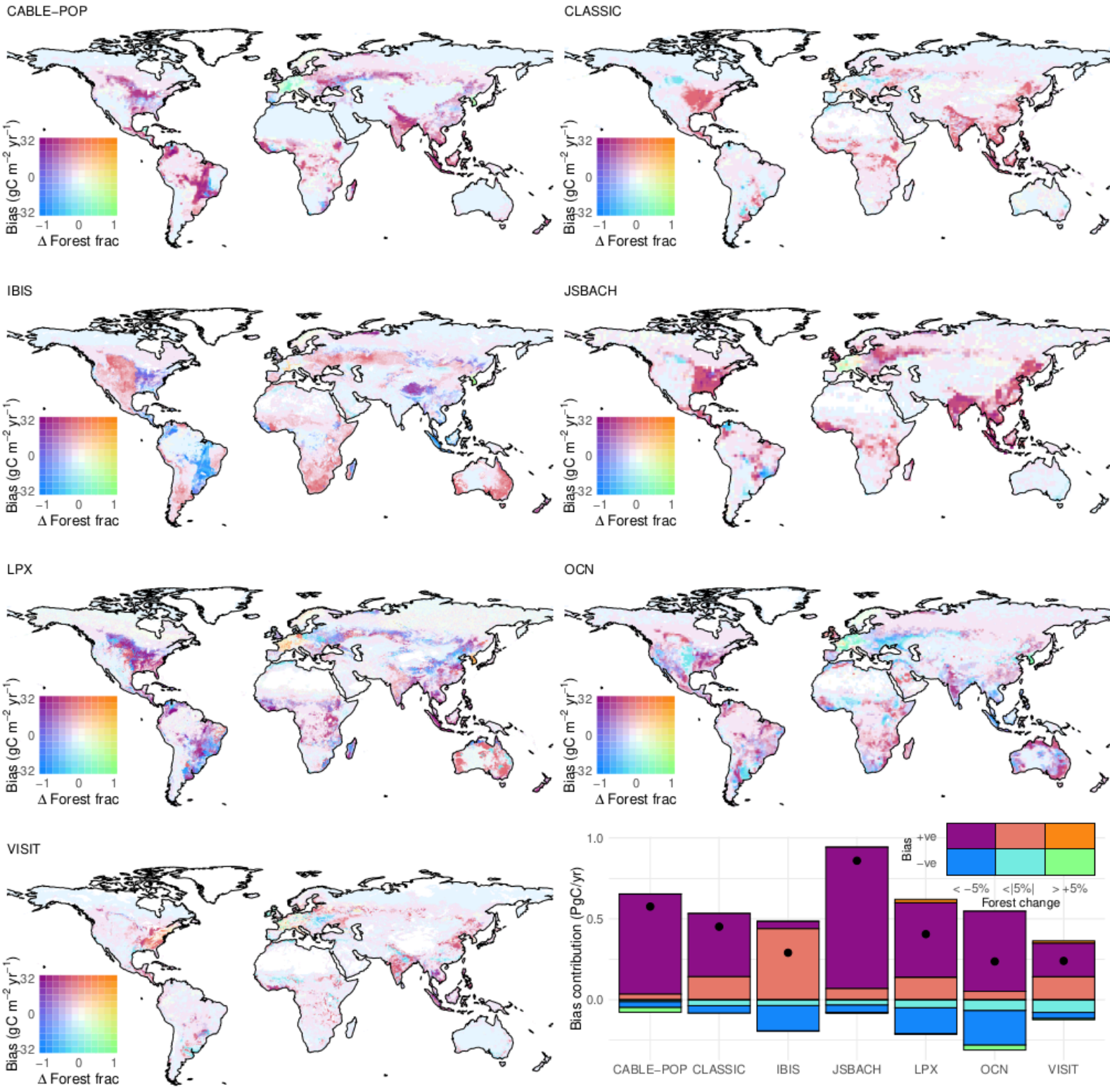

Supplementary Figure 3 - Forest cover loss predominantly explains the model bias in the natural land sink (SLAND). Maps show the carbon flux bias (RSS; gC m^{-2} yr^{-1}) for the seven DGVMs, averaged over 2014-2023, plotted as a bivariate colour map against forest fraction change from 1700 to 2023 (ΔForest frac) from the simulation with transient land use change.

Purple colors indicate regions where forest loss substantially contributes to the overestimation of the natural land sink. The bar chart shows the contribution of six 'forest change - sink bias' combinations to the global mean RSS bias (PgC yr^{-1}) for each model, calculated from the gridcell data. Colours correspond to combinations of forest cover change (≤-5%, -5% to +5%, ≥+5%) and flux bias sign (positive or negative). Black dots indicate the net global RSS bias per model.

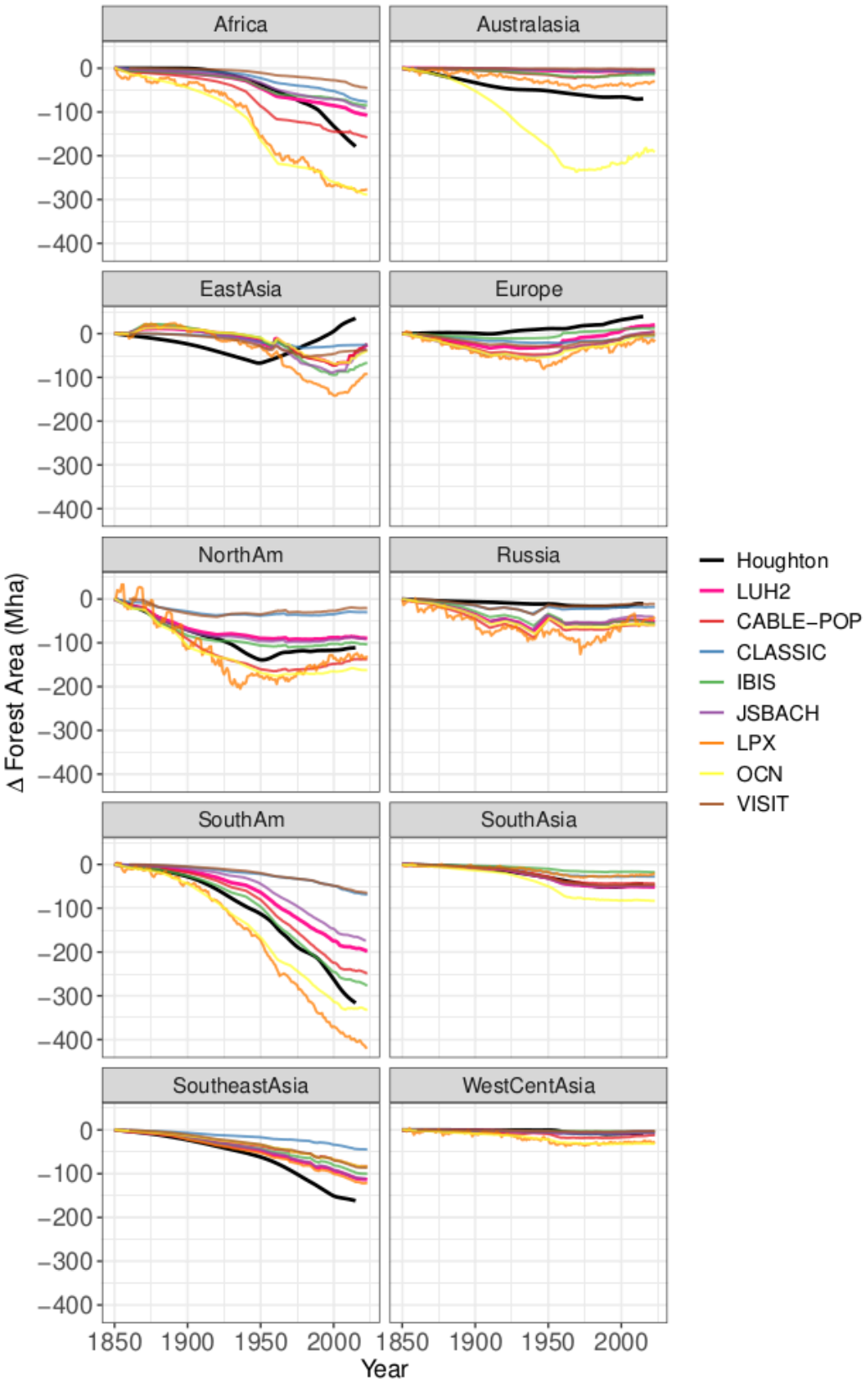

Supplementary Figure 4 - Changes in forest areas are highly uncertain. Regional change in forest areas since 1850 from reconstructions (Houghton, LUH2) and simulated by the seven DGVMs used to estimate RSS.

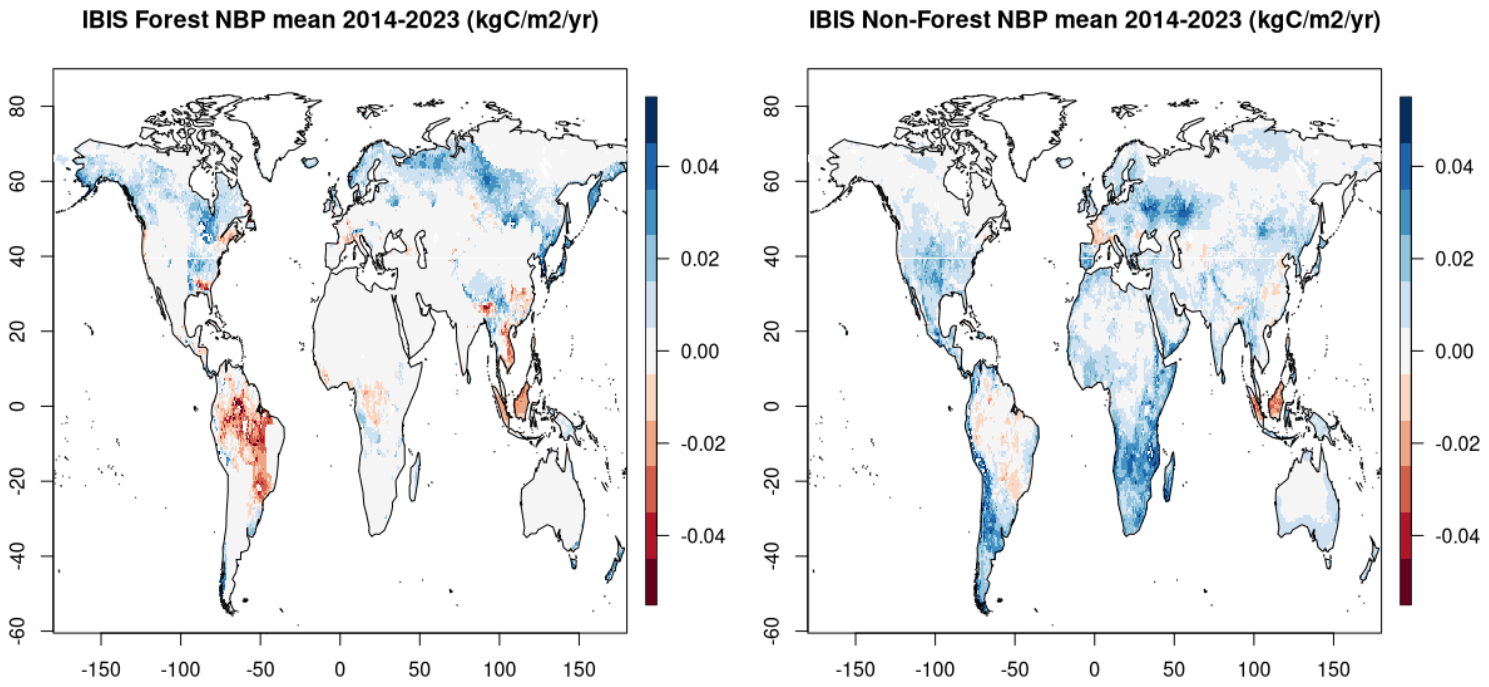

Supplementary Figure 5 - Maps showing SLAND (kgC m-2 yr-1) for IBIS for forest PFTs and non-forest PFTs averaged over 2014-2023.

References

1. Reick, C. H., Raddatz, T., Brovkin, V. & Gayler, V. Representation of natural and anthropogenic land cover change in MPI-ESM: Land Cover in MPI-ESM. *J. Adv. Model. Earth Syst.* **5**, 459–482 (2013).
2. Pongratz, J. *et al.* Land use effects on climate: Current state, recent progress, and

emerging topics. *Curr. Clim. Change Rep.* **7**, 99–120 (2021).

3. de Noblet-Ducoudré, N. *et al.* Determining Robust Impacts of land-use-induced land cover changes on surface climate over North America and Eurasia: Results from the first set of LUCID experiments. *J. Clim.* **25**, 3261–3281 (2012).
4. Chini, L. *et al.* Land-use harmonization datasets for annual global carbon budgets. *Earth Syst. Sci. Data* **13**, 4175–4189 (2021).
5. Hurtt, G. C. *et al.* Harmonization of global land use change and management for the period 850–2100 (LUH2) for CMIP6. *Geosci. Model Dev.* **13**, 5425–5464 (2020).
6. Houghton, R. A. & Castanho, A. Annual emissions of carbon from land use, land-use change, and forestry 1850–2020. (2022) doi:10.5194/essd-2022-351.
7. Friedlingstein, P. *et al.* Global carbon budget 2024. *Earth Syst. Sci. Data* **17**, 965–1039 (2025).
8. Sitch, S. *et al.* Trends and drivers of terrestrial sources and sinks of carbon dioxide: An overview of the TRENDY project. *Global Biogeochem. Cycles* **38**, (2024).
9. Amali, A. A. *et al.* Biogeochemical versus biogeophysical temperature effects of historical land-use change in CMIP6. (2024) doi:10.5194/egusphere-2024-2460.
10. Pongratz, J. *et al.* Chapter 7: Current levels of CDR, the state of carbon dioxide removal - 2nd edition. Preprint at https://doi.org/10.17605/OSF.IO/ZXSKB (2024).
11. Canadell, J. G. *et al.* From global to national GHG budgets: the REgional Carbon Cycle Assessment and Processes-3 (RECCAP3). *Natl. Sci. Rev.* **12**, nwaf037 (2025).
12. Grassi, G. *et al.* Improving land-use emission estimates under the Paris Agreement. *Nat. Sustain.* (2025) doi:10.1038/s41893-025-01565-1.
13. Schwingshackl, C. *et al.* Differences in land-based mitigation estimates reconciled by separating natural and land-use CO2 fluxes at the country level. *One Earth* **5**, 1367–1376 (2022).